International Workshop on Advanced Motion Control, pp. 74 - 79, 2000.

Proposal of Seeking Control of Hard Disk Drives Based on Perfect Tracking Control using Multirate Feedforward Control

Hiroshi Fujimoto† Yoichi Hori† Takashi Yamaguchi‡ Shinsuke Nakagawa‡

†Dept. Electrical Eng., The Univ. of Tokyo, 7-3-1 Hongo, Bunkyo, Tokyo, 113-8656 Japan
tel:+81-3-5841-7683; fax:+81-3-5841-7687; e-mail:fuji@hori.t.u-tokyo.ac.jp
‡Mech. Eng. Research Lab., Hitachi, Ltd.

Abstract: In this paper, novel multirate two-degree-of-freedom controllers are proposed for digital control systems, where it is restricted that the speed of the A/D converters are slower than that of the D/A converters. The proposed feedforward controller assures the perfect tracking at M inter-sampling points. Moreover, it is shown that the structure of the proposed perfect tracking controller is very simple and clear. Next, the proposed method is extended to systems with time delay. The proposed scheme is applied to the seeking control for hard disk drive, and advantages of this approach are demonstrated by simulations and experiments.

1 Introduction

Head-positioning controllers of hard disk drives are generally composed of two control modes; the track-seeking mode and the track-following mode. In the track-seeking mode, the feedforward performance is important because the head is moved to the desired track as fast as possible. After that, the head needs to be positioned on the desired track while the information is read or written. In the track-following mode, the disturbance rejection performance is important because the head must be positioned finely on the desired track under the vibrations generated by the disk rotation and disturbance. In the long-span seeking, where the seeking distance is comparatively long, high speed seeking is achieved by the mode-switching controller [1]. In the short-span seeking, however, single mode controllers based on two-degree-of-freedom control have advantages, because the mode-switching controller sometimes generates undesirable transient response [2, 3, 4].

Digital two-degree-of-freedom controllers generally have two samplers for the reference signal $r(t)$ and the output $y(t)$, and one holder on the input $u(t)$ as shown in Fig. 2. Therefore, there exist three time periods T_r, T_y, and T_u which represent the period of $r(t), y(t)$, and $u(t)$, respectively. The input period T_u is generally decided by the speed of the actuator, D/A converter, or the calculation on the CPU. Moreover, the output period T_y is also determined by the speed of the sensor or the A/D converter.

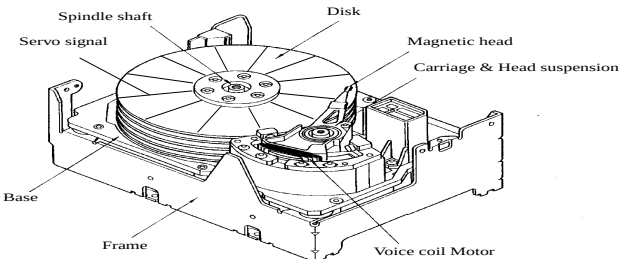

Fig.1: Hard disk drive.

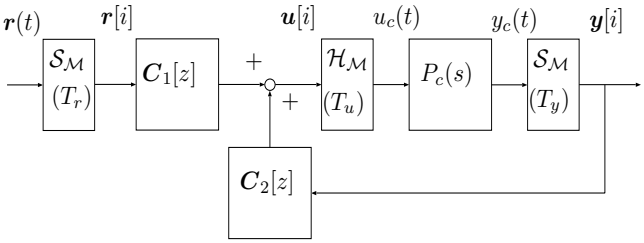

Fig.2: Two-degree-of-freedom control system.

In the head-positioning control of hard disk drives, the head position is detected by the discrete servo signals embedded in the disks as shown in Fig. 1. Therefore, the output sampling period T_y is decided by the number of these signals and the rotation frequency of the spindle motor. However, it is possible to set the control period T_u shorter than T_y because of the recent development of CPU. Thus, the controller can be regarded as the multirate control system which have the hardware restriction of $T_u < T_y$.

In this paper, the digital control systems which have the hardware restrictions of $T_u < T_y$ are assumed, and novel design method of multirate feedforward controller is proposed, which achieve the perfect tracking at M inter-sample points of T_y. Next, the proposed method is extended to systems with time delay. The restriction of $T_u < T_y$ may be general because D/A converters are usually faster than the A/D converters. Multirate controllers also have demonstrated higher performance both in feedforward [2, 3] and feedback [5, 6] characteristics. In this paper, the proposed perfect tracking controller is applied to the track-seeking mode of HDD.

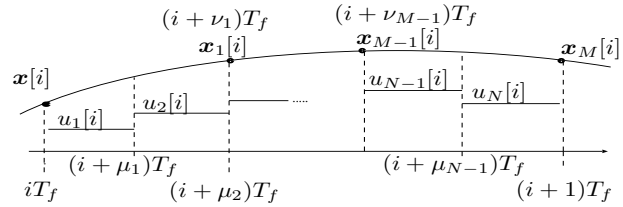

Fig.3: Multirate sampling control.

2 Design of the perfect tracking controller

In the conventional digital tracking control systems, it is impossible to track the desired trajectory with zero error [7], because the discrete-time plant discretized by the zero-order-hold usually has unstable zeros [8].

The unstable zeros problems of the discrete-time plant have been resolved by zero assignment method in use of multirate input control in [9] and [10]. However, [11] shows that those methods have disadvantages of large overshoot and oscillation in the inter-sample points because the control input changes back and forth very quickly. On the other hand, [12] proposed the perfect tracking control by introducing the multirate feedforward control, which never has this problem because all of the plant states are controlled along the smoothed desired trajectories.

In this section, new multirate feedforward controller is proposed. For the restriction of $T_u < T_y$, the flame period T_f is defined as $T_f = T_y$, and the dynamics of the controller is described by T_f. In this paper, the integer M is selected so as to $M \triangleq N/n$ becomes an integer, where N is the input multiplicity and n is the plant order. As shown in Fig. 3, the plant input is changed N times during $T_y(= T_f)$, and the perfect tracking of the plant state is guaranteed M times during T_y.

For simplification, the continuous-time plant is assumed to be SISO system in this paper. The proposed methods, however, can be extended to deal with the MIMO system by the same way as [13].

2.1 Plant Discretization by Multirate Sampling

Consider the continuous-time plant described by

$$\dot{\boldsymbol{x}}(t) = \boldsymbol{A_c}\boldsymbol{x}(t) + \boldsymbol{b_c}u(t)\ ,\quad y(t) = \boldsymbol{c}_c\boldsymbol{x}(t). \tag{1}$$

The discrete-time plant discretized by the multirate sampling control (Fig. 3) becomes

$$\boldsymbol{x}[i+1] = \boldsymbol{A}\boldsymbol{x}[i] + \boldsymbol{B}\boldsymbol{u}[i]\ ,\quad y[i] = \boldsymbol{C}\boldsymbol{x}[i], \tag{2}$$

where $\boldsymbol{x}[i] = \boldsymbol{x}(iT)$, and where matrices $\boldsymbol{A}, \boldsymbol{B}, \boldsymbol{C}$ and vectors $\boldsymbol{u}$ are given by

$$\left[\begin{array}{c|c} \boldsymbol{A} & \boldsymbol{B} \\ \hline \boldsymbol{C} & \boldsymbol{O} \end{array}\right] \triangleq \left[\begin{array}{c|ccc} e^{\boldsymbol{A_c}T_f} & \boldsymbol{b}_1 & \cdots & \boldsymbol{b}_N \\ \hline \boldsymbol{c}_c & 0 & \cdots & 0 \end{array}\right], \tag{3}$$

$$\boldsymbol{b}_j \triangleq \int_{(1-\mu_j)T_f}^{(1-\mu_{(j-1)})T_f} e^{\boldsymbol{A_c}\tau}\boldsymbol{b_c}d\tau\ ,\ \boldsymbol{u} \triangleq [u_1, \cdots, u_N]^T, \tag{4}$$

$$0 = \mu_0 < \mu_1 < \mu_2 < ... < \mu_N = 1. \tag{5}$$

The inter-sample plant state at $t = (i+\nu_k)T_f$ is represented by

$$\tilde{\boldsymbol{x}}[i] = \tilde{\boldsymbol{A}}\boldsymbol{x}[i] + \tilde{\boldsymbol{B}}\boldsymbol{u}[i], \tag{6}$$

$$\left[\ \tilde{\boldsymbol{A}}\ \middle|\ \tilde{\boldsymbol{B}}\ \right] \triangleq \left[\begin{array}{c|ccc} \tilde{\boldsymbol{A}}_1 & \tilde{\boldsymbol{b}}_{11} & \cdots & \tilde{\boldsymbol{b}}_{1N} \\ \vdots & \vdots & & \vdots \\ \tilde{\boldsymbol{A}}_M & \tilde{\boldsymbol{b}}_{M1} & \cdots & \tilde{\boldsymbol{b}}_{MN} \end{array}\right], \tag{7}$$

$$\tilde{\boldsymbol{A}}_k \triangleq e^{\boldsymbol{A_c}\nu_k T_f},\ \tilde{\boldsymbol{x}} \triangleq [\boldsymbol{x}_1^T, \cdots, \boldsymbol{x}_M^T]^T, \tag{8}$$

$$\boldsymbol{x}_k[i] = \boldsymbol{x}[i+\nu_k] = \boldsymbol{x}((i+\nu_k)T_f), \tag{9}$$

$$\tilde{\boldsymbol{b}}_{kj} \triangleq \left\{\begin{array}{cc} \mu_j < \nu_k : & \int_{(\nu_k-\mu_j)T_f}^{(\nu_k-\mu_{(j-1)})T_f} e^{\boldsymbol{A_c}\tau}\boldsymbol{b_c}d\tau \\ \mu_{(j-1)} < \nu_k \le \mu_j : & \int_0^{(\nu_k-\mu_{(j-1)})T_f} e^{\boldsymbol{A_c}\tau}\boldsymbol{b_c}d\tau \\ \nu_k \le \mu_{(j-1)} : & 0 \end{array}\right.,$$

$$0 < \nu_1 < \nu_2 < ... < \nu_M = 1, \tag{10}$$

where $\mu_j (j = 0, 1, \cdots, N)$ and $\nu_k (k = 1, \cdots, M)$ are the parameters for multirate sampling as shown in Fig. 3. If T_f is divided at same intervals, $\mu_j = j/N, \nu_k = k/M$.

2.2 Design of the perfect tracking controller

In this section, the perfect tracking controller $\boldsymbol{C}_1[z]$ is designed so that the plant state ($\boldsymbol{x}$) completely tracks the desired trajectory ($\boldsymbol{x}^*$) at every sampling points $T_r(= T_y/M)$ [12].

Before the perfect tracking controller $\boldsymbol{C}_1[z]$ is designed, the feedback controller $\boldsymbol{C}_2[z]$ has to be determined. Here, the $\boldsymbol{C}_2[z]$ must be a robust controller which let the sensitivity function $\boldsymbol{S}[z] = (\boldsymbol{I} - \boldsymbol{P}[z]\boldsymbol{C}_2[z])^{-1}$ be small enough in the frequency of the desired trajectory. The reason is that the sensitivity function $\boldsymbol{S}[z]$ represents the variation of the command response $\boldsymbol{G}_{yr}[z]$ under the variation of $\boldsymbol{P}[z]$ [14].

This paper adopts the simplest feedback controller $\boldsymbol{C}_2[z]$, which is obtained from a conventional single-rate controller such as a disturbance observer or H_∞ controller. In this case, the outputs of the $\boldsymbol{C}_2[z]$ become the same values during one sampling period T_y as represented by

$$\boldsymbol{C}_2[z] = \left[\begin{array}{c|c} \boldsymbol{A}_s & \boldsymbol{b}_s \\ \hline \boldsymbol{c}_s & d_s \\ \vdots & \vdots \\ \boldsymbol{c}_s & d_s \end{array}\right], \tag{11}$$

where $\{\boldsymbol{A}_s, \boldsymbol{b}_s, \boldsymbol{c}_s, d_s\}$ is a single-rate controller designed on T_y. Furthermore, the multirate feedback controller can improve the stability margin [5] and disturbance rejection performance of the inter-sample response [15].

The control law of Fig. 2 is described by

$$\boldsymbol{u} = \boldsymbol{C}_1\boldsymbol{r} + \boldsymbol{C}_2 y \tag{12}$$

$$= \boldsymbol{F}\hat{\boldsymbol{x}} + \boldsymbol{Q}e_y + \boldsymbol{K}\boldsymbol{r}, \tag{13}$$

where $\boldsymbol{K}, \boldsymbol{Q} \in \boldsymbol{RH}_\infty$ are free parameters [16]. Therefore, Fig. 2 can be transferred to Fig. 4. In the figure, $\mathcal{H}_\mathcal{M}$, $\mathcal{S}$, and the thick lines represent the multirate hold,

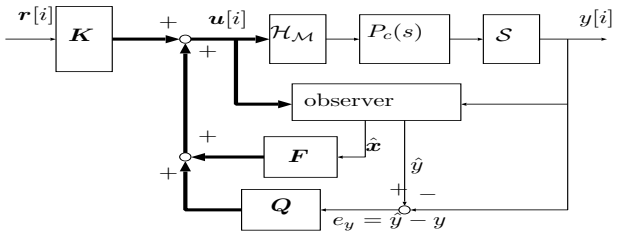

Fig.4: Basic structure of TDOF control.

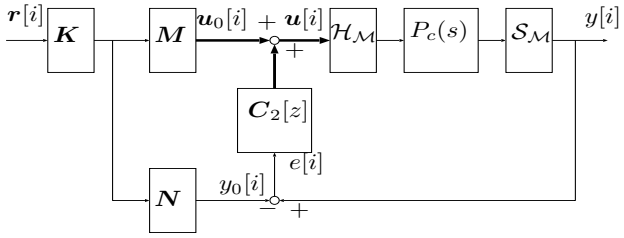

Fig.5: Implementation of the proposed controller.

the sampler, and the multirate signals, respectively. In this paper, $\boldsymbol{K}$ becomes a constant matrix.

Because the estimation errors of the observer become zero ($\hat{\boldsymbol{x}} = \boldsymbol{x}, e_y = 0$) for the nominal plant, from (6) and (13), this system is represented by

$$\tilde{\boldsymbol{x}}[i] = (\tilde{\boldsymbol{A}} + \tilde{\boldsymbol{B}}\boldsymbol{F})\boldsymbol{x}[i] + \tilde{\boldsymbol{B}}\boldsymbol{K}\boldsymbol{r}[i]. \tag{14}$$

Because non-singularity of the matrix $\tilde{\boldsymbol{B}}$ can be assured by $Mn = N$ and $T_r = nT_u$ [12, 17], the coefficient matrices of (14) can be arbitrary assigned by $\boldsymbol{F}$ and $\boldsymbol{K}$. In this paper, the parameters $\boldsymbol{F}$ and $\boldsymbol{K}$ can be selected so that following equations are satisfied.

$$\tilde{\boldsymbol{A}} + \tilde{\boldsymbol{B}}\boldsymbol{F} = \boldsymbol{O}\ , \quad \tilde{\boldsymbol{B}}\boldsymbol{K} = \boldsymbol{I} \tag{15}$$

From (15), $\boldsymbol{F}$ and $\boldsymbol{K}$ are given by

$$\boldsymbol{F} = -\tilde{\boldsymbol{B}}^{-1}\tilde{\boldsymbol{A}}\ , \quad \boldsymbol{K} = \tilde{\boldsymbol{B}}^{-1}. \tag{16}$$

Therefore, (14) is described by $\tilde{\boldsymbol{x}}[i] = \boldsymbol{r}[i]$. Utilizing the future inter-sample desired state $\tilde{\boldsymbol{x}}^*[i]$, if the reference input is set to $\boldsymbol{r}[i] = \tilde{\boldsymbol{x}}^*[i]$ with the preview action, we find the perfect tracking $\tilde{\boldsymbol{x}}[i] = \tilde{\boldsymbol{x}}^*[i]$ can be achieved at every sampling point T_r.

Because $\boldsymbol{C}_1[z]$ of (12) can be transferred to (17), $\boldsymbol{C}_1[z]$ is given by (Fig. 5)

$$\boldsymbol{C}_1[z] = (\boldsymbol{M} - \boldsymbol{C}_2\boldsymbol{N})\boldsymbol{K}, \tag{17}$$

$$\begin{aligned} \boldsymbol{M} &= \left[\begin{array}{c|c} \boldsymbol{A}+\boldsymbol{B}\boldsymbol{F} & \boldsymbol{B} \\ \hline \boldsymbol{F} & \boldsymbol{I} \end{array}\right] = \boldsymbol{I} + z^{-1}\boldsymbol{F}\boldsymbol{B}, \\ \boldsymbol{N} &= \left[\begin{array}{c|c} \boldsymbol{A}+\boldsymbol{B}\boldsymbol{F} & \boldsymbol{B} \\ \hline \boldsymbol{C} & \boldsymbol{O} \end{array}\right] = z^{-1}\boldsymbol{C}\boldsymbol{B}, \end{aligned} \tag{18}$$

where $\boldsymbol{M}, \boldsymbol{N}$ are the right coprime factorization of the plant $\boldsymbol{P}[z] = \boldsymbol{N}\boldsymbol{M}^{-1}$[14].

Next, it is shown that the structure of the perfect tracking controller is very simple and clear. [18] shows that the structure of the proposed controller is represented by Fig. 6. The plant $\boldsymbol{P}[z]$ is driven by the stable inverse system. When the tracking error $e[i]$ is generated

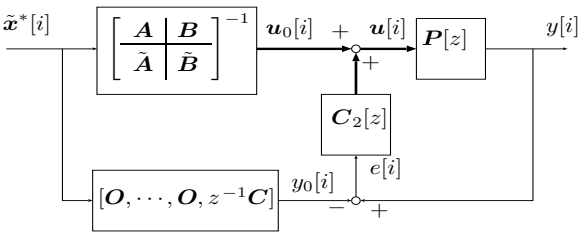

Fig.6: Structure of the proposed controller.

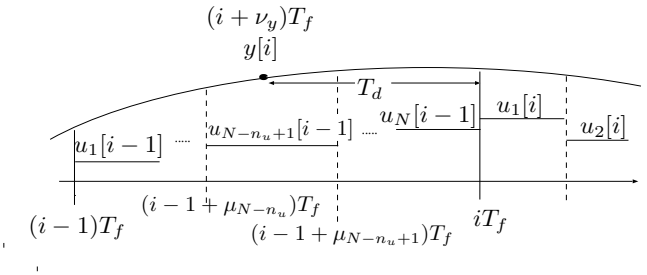

Fig.7: Time chart of the time delay.

by disturbance or modeling error, the robust feedback controller $\boldsymbol{C}_2[z]$ works in order to compensate the error $e[i]$.

2.3 Extension to system with time delay

In this section, the proposed perfect tracking control is extended to plants with time delay. As shown in Fig. 7, the time delay is considered to exist on the plant output. The continuous-time plant with time delay T_d is described by

$$\dot{\boldsymbol{x}}(t) = \boldsymbol{A}_{\boldsymbol{c}}\boldsymbol{x}(t) + \boldsymbol{b}_{\boldsymbol{c}}u(t)\ , \quad y(t) = \boldsymbol{c}_c\boldsymbol{x}(t - T_d). \tag{19}$$

The time delay can also be considered to exist on the plant input, and expressed by [19]

$$\dot{\boldsymbol{x}}(t) = \boldsymbol{A}_{\boldsymbol{c}}\boldsymbol{x}(t) + \boldsymbol{b}_{\boldsymbol{c}}u(t - T_d)\ , \quad y(t) = \boldsymbol{c}_c\boldsymbol{x}(t). \tag{20}$$

However, in case of the single input and single output plant, (19) is equivalent to (20). Thus, this paper adopts (19) because it can make this extension more simple theoretically. Moreover, the time delay is assumed to be $T_d \le T_f$ for simplification. The proposed methods, however, can be extended to the time delay of $T_d > T_f$ by the same way as [19].

Discretizing (20) by the multirate sampling control (Fig. 7), the discrete-time plant becomes

$$\bar{\boldsymbol{x}}[i+1] = \bar{\boldsymbol{A}}\bar{\boldsymbol{x}}[i] + \bar{\boldsymbol{B}}\boldsymbol{u}[i], \tag{21}$$

$$y[i] = \bar{\boldsymbol{c}}\ \bar{\boldsymbol{x}}[i], \tag{22}$$

$$\bar{\boldsymbol{A}} \triangleq \left[\begin{array}{cc} \boldsymbol{A} & \boldsymbol{O} \\ \boldsymbol{O} & \boldsymbol{O} \end{array}\right],\ \bar{\boldsymbol{B}} \triangleq \left[\begin{array}{c} \boldsymbol{B} \\ \boldsymbol{E} \end{array}\right],\ \bar{\boldsymbol{x}} \triangleq \left[\begin{array}{c} \boldsymbol{x} \\ \boldsymbol{x}_u \end{array}\right], \tag{23}$$

$$\bar{\boldsymbol{c}} \triangleq [\boldsymbol{c}|\boldsymbol{d}] = [\boldsymbol{c}_c e^{\boldsymbol{A}_{\boldsymbol{c}}\nu_y T_f}|\boldsymbol{d}_{N-n_u+1}, \cdots, \boldsymbol{d}_N], \tag{24}$$

Table 1: Plant's parameters.

Amplifier gain	K_a	1.996	A/V
Force constant	K_f	2.95	N/A
Mass	M_p	6.983	g
Track pitch	T_p	3.608	μm/trk
Sampling time	T_s	138.54	μsec
Calculation delay	T_{calc}	38	μsec
Equivalent delay	T_{equiv}	38.7	μsec
Input multiplicity	N	4	

$$\boldsymbol{d}_j \triangleq \begin{cases} \nu_y \le -1+\mu_{(j-1)} : \\ \quad -\boldsymbol{c}_c e^{\boldsymbol{A_c}\nu_y T_f}\int_{(1-\mu_j)T_f}^{(1-\mu_{(j-1)})T_f} e^{\boldsymbol{A_c}\tau}\boldsymbol{b_c}d\tau \\ -1+\mu_{(j-1)} \le \nu_y < -1+\mu_j : \\ \quad -\boldsymbol{c}_c e^{\boldsymbol{A_c}\nu_y T_f}\int_{(1-\mu_j)T_f}^{-\nu_y T_f} e^{\boldsymbol{A_c}\tau}\boldsymbol{b}_c d\tau \\ -1+\mu_j \le \nu_y < 0 : 0 \end{cases}, \quad (25)$$

$$\boldsymbol{E} \triangleq [\boldsymbol{O}, \boldsymbol{I}_{n_u}], \quad \nu_y = -\frac{T_d}{T_f}, \quad (26)$$

where n_u is a number of the of $\boldsymbol{u}[i-1]$ elements during T_d as shown in Fig. 7, and $\boldsymbol{x}_u$ is a vector composed of these elements.

The exact plant model with time delay is obtained by (21) and (22). Moreover, $\boldsymbol{F}$ and $\boldsymbol{K}$ obtained in (16) guarantee the perfect tracking, if the model $\boldsymbol{P}[z] = \boldsymbol{N}\boldsymbol{M}^{-1}$ in the proposed feedforward controller includes the time delay. Therefore, from (21) and (22), the proposed controller is extended to the plants with time delay by

$$\boldsymbol{C}_1[z] = (\boldsymbol{M} - \boldsymbol{C}_2\boldsymbol{N})\boldsymbol{K}, \quad (27)$$

$$\boldsymbol{M} = \left[\begin{array}{c|c} \bar{\boldsymbol{A}}+\bar{\boldsymbol{B}}\bar{\boldsymbol{F}} & \bar{\boldsymbol{B}} \\ \hline \boldsymbol{F} & \boldsymbol{I} \end{array}\right], \boldsymbol{N} = \left[\begin{array}{c|c} \bar{\boldsymbol{A}}+\bar{\boldsymbol{B}}\bar{\boldsymbol{F}} & \bar{\boldsymbol{B}} \\ \hline \bar{\boldsymbol{c}} & \boldsymbol{O} \end{array}\right] \quad (28)$$

$$\bar{\boldsymbol{F}} = [\boldsymbol{F}, \boldsymbol{O}]. \quad (29)$$

3 Applications to HDD

3.1 Modeling of the plant

The experimental setup is 3.5-in hard disk drive. Let the nominal model of this plant be

$$P_c(s) = \frac{K_f K_a}{M_p s^2} e^{-sT_d}. \quad (30)$$

The parameters of this plant are shown in Table 1. While servo signals are detected at a constant period about 138 [μs], the control input can be changed 4 times. Therefore, the proposed approach is applicable. In the experiment, the time delay $T_d = T_{calc} + T_{equiv}$ is considered, where T_{calc} is the calculation delay of the processor, and T_{equiv} is the equivalent delay of the current control and the notch filter for the second mechanical resonance mode. The actual plant has the first mechanical resonance mode around 2.7 [kHz]. The Nyquist frequency is also 3.6 [kHz]. In spite of those, the target seeking-time is set to 3 sampling time (2.4 [kHz]) for one track seeking in these experiments.

Table 2: Parameters of the trajectories.

	A_r[trk]	$f_r(=1/2\pi\tau_r)$ [kHz]
Condition A	1	2.8
Condition B	6	1.7

3.2 Applications of perfect tracking controller to seeking mode

The perfect tracking controller is designed on input multiplicity $N = 4$. Because the plant is second order system ($n = 2$), the perfect tracking is assured $N/n = 2$ times at every sampling points. In the following simulations and experiments, the proposed method is compared with ZPETC proposed in [7]. ZPETC is one of the most well-known and important feedforward controllers in the mechanical system control. [3] and [4] applied it to the hard disk drive control.

The control period T_u of ZPETC becomes four times as long as that of the proposed method because ZPETC is single-rate controller[1] and two methods are compared at same sampling period T_y. The feedback controllers of two methods are same single-rate PI-Lead filters. Moreover, the desired trajectory (31) is selected, which jurk (differential acceleration) is smooth in order not to excite the mechanical resonance mode.

$$y^*(s) = \frac{A_r}{s(\tau_r s+1)^4} e^{-sT_d} \quad (31)$$

$$v^*(s) = \frac{A_r}{(\tau_r s+1)^4} e^{-sT_d} \quad (32)$$

The parameters of these desired trajectories are shown in Table 2. In these experiments, the multirate feedforward input $\boldsymbol{u}_0[i]$ in Fig. 5 and 6 is obtained by off-line calculation in order to save the processor resources. Therefore, the order of the feedforward controller and the desired trajectory are not related to the calculation time delay.

3.2.1 Simulation results

Simulation results are shown in Fig. 8 and 9. Fig. (a) and (b) show that the proposed method gives better performance than ZPETC. While the response of ZPETC has large tracking error caused by the unstable zero, that of the proposed method has almost zero tracking error. Fig. (c) also indicates that the proposed multirate input is very smooth.

The frequency responses from the desired trajectory $y_d[i]$ to the output $y[i]$ are shown in Fig. 10. Because the proposed method (PTC) assures the perfect tracking, the command response becomes 1 in the all frequency. However, the gain of ZPETC decreases in the high frequency. The frequency of the short-span seeking is 2 [kHz] around. Therefore, the proposed method has advantages in seeking control.

[1] [3, 20] attempt to extend ZPETC to multirate controllers.

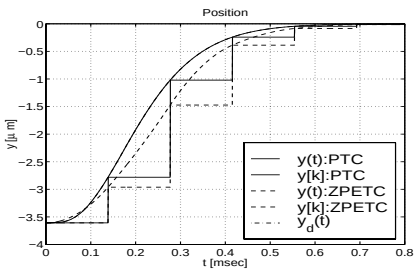

(a) Position

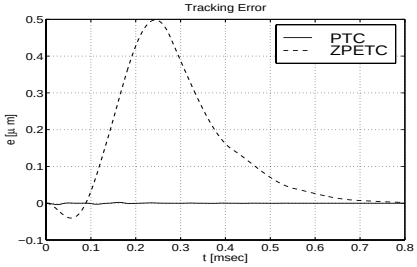

(b) Tracking error

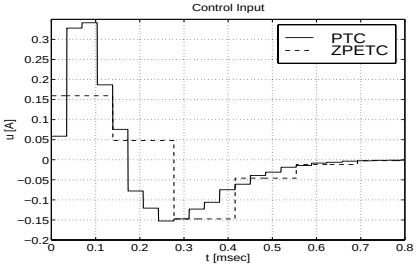

(c) Control input

Fig.8: Simulation results A (1trk).

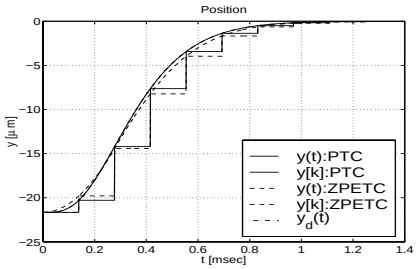

(a) Position

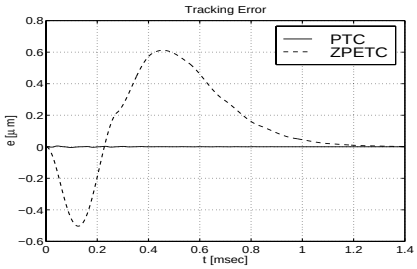

(b) Tracking error

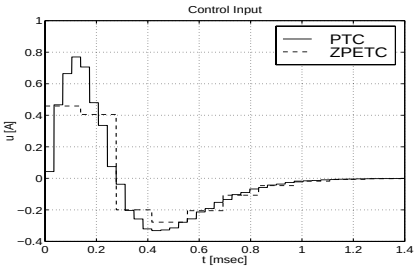

(c) Control input

Fig.9: Simulation results B (6trk).

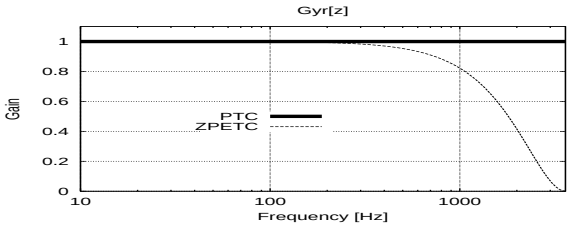

Fig.10: Frequency responses ($y[z]/y^*[z]$).

3.2.2 Experimental results

Experimental results are shown Fig. 11 and 12. In Fig. (a), about 1,000 experimental data are overwritten. Fig. (b) and (c) are averages of them, which show the proposed method has high tracking performance. Although the actual plant has mechanical resonance mode around 2.7 [kHz], this mode is not suppressed by notch filter in order to save the phase margin. In spite of that, the experiment of condition A (1 [trk]) adopts the wide bandwidth desired trajectory ($f_r = 2.8$ [kHz]) for high speed seeking. Therefore, Fig. 11(a)(b) have overshoot of maximum height 0.4 [μm]. However, this overshoot is in permissible range because the overshoot is small enough compared with the track pitch 3.6 [μm].

Because the position signal is detectable only on the sampling points, the comparison results between the proposed method and ZPETC are not clear in Fig. 11 and 12. Therefore, in this section, the proposed method is compared by the average of the seeking-time measured in the 2000 times experiments. The seeking-time is defined as the time from the seeking start to the point when the remaining distance becomes under 0.4 [μm] and the overshoot is smaller than 0.4 [μm].

Table 3: Experimental seeking-time.

	PTC [ms]	ZPETC [ms]	Conventional [ms]
A 1trk	0.4394 ($3.17T_s$)	0.5226 ($3.77T_s$)	0.5738 ($4.14T_s$)
B 6trk	1.200 ($8.66T_s$)	1.325 ($9.57T_s$)	1.933 ($14.0T_s$)

Table 3 shows the average seeking-time which obtained in the experiments. The seeking-time of the proposed method (PTC) is much smaller than that of ZPETC and the conventional settling control [1]. In the short-span seeking (1 [trk]), the seeking-time of the proposed method is 19 and 31 [%] shorter than the ZPETC and conventional method, respectively. In the middle-span seeking (6 [trk]), the proposed method is 1 and 6 sampling time faster than them.

4 Conclusion

In this paper, the digital control systems which have hardware restrictions of $T_u < T_y$ were assumed, the multirate feedforward controller was proposed, which assures the perfect tracking at M inter-sample points. It was shown that the structure of the proposed perfect tracking controller was very simple and clear. Next, the proposed method was extended to systems with time delay.

Moreover, the proposed method was applied to the track-seeking mode of the hard disk drive. The advantages of this approach were demonstrated by the simulations and experiments.

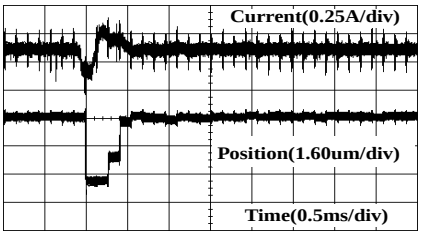

(a) 1000 times seeking

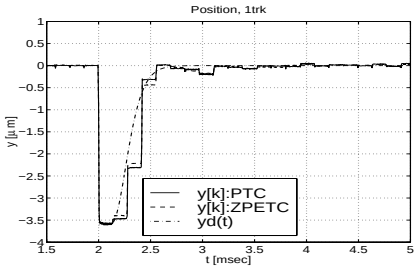

(b) Position (average)

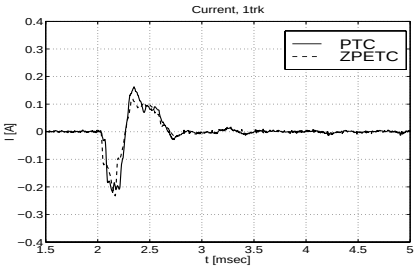

(c) Current (average)

Fig.11: Experimental results A (1trk).

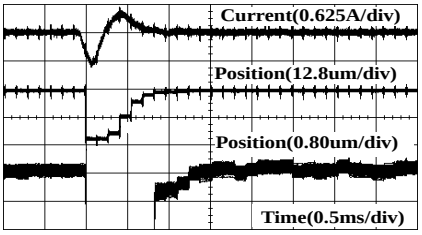

(a) 1000 times seeking

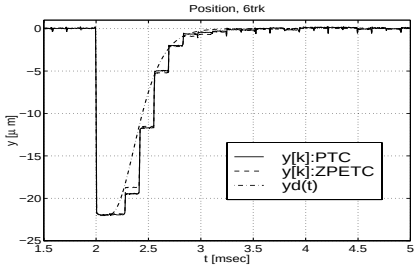

(b) Position (average)

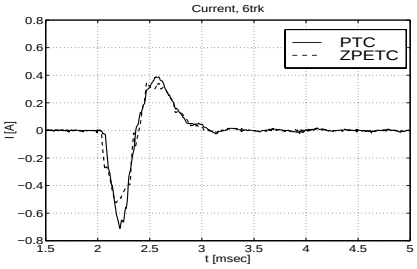

(c) Current (average)

Fig.12: Experimental results B (6trk).

Finally, the authors would like to note that part of this research is carried out with a subsidy of the Scientific Research Fund of the Ministry of Education.

References

[1] T. Yamaguchi, H. Numasato, and H. Hirai, "A mode-switching control for motion control and its application to disk drives: Design of optimal mode-switching conditions," *IEEE/ASME Trans. Mechatronics*, vol. 3, no. 3, pp. 202–209, 1998.

[2] S. Takakura, "Design of the tracking system using N-Delay two-degree-of-freedom control and its application to hard disk drives," in *IEEE Conf. Control Applications*, pp. 170–175, August 1999.

[3] M. Kobayashi, T. Yamaguchi, I. Oshimi, Y. Soyama, Y. Hara, and H. Hirai, "Multirate zero phase error feedforward control for magnetic disk drives," in *JSME, IIP '98*, pp. 21–22, August 1998. (in Japanese).

[4] L. Yi and M. Tomizuka, "Two-degree-of-freedom control with robust feedback control for hard disk servo systems," *IEEE/ASME Trans. Mechatronics*, vol. 4, no. 1, pp. 17–24, 1999.

[5] W.-W. Chiang, "Multirate state-space digital controller for sector servo systems," in *Conf. Decision Contr.*, pp. 1902–1907, 1990.

[6] T. Hara and M. Tomizuga, "Performance enhancement of multi-rate controller for hard disk drives," *IEEE Trans. Magnetics*, vol. 35, no. 2, pp. 898–903, 1999.

[7] M. Tomizuka, "Zero phase error tracking algorithm for digital control," *ASME, J. Dynam. Syst., Measur., and Contr.*, vol. 109, pp. 65–68, March 1987.

[8] K. J. Åström, P. Hangander, and J. Sternby, "Zeros of sampled system," *Automatica*, vol. 20, no. 1, pp. 31–38, 1984.

[9] P. T. Kabamba, "Control of linear systems using generalized sampled-data hold functions," *IEEE Trans. Automat. Contr.*, vol. 32, no. 9, pp. 772–783, 1987.

[10] T. Mita, Y. Chida, Y. Kazu, and H. Numasato, "Two-delay robust digital control and its applications – avoiding the problem on unstable limiting zeros," *IEEE Trans. AC*, vol. 35, no. 8, pp. 962–970, 1990.

[11] K. L. Moore, S. P. Bhattacharyya, and M. Dahleh, "Capabilities and limitations of multirate control schemes," *Automatica*, vol. 29, no. 4, pp. 941–951, 1993.

[12] H. Fujimoto, Y. Hori, and A. Kawamura, "High performance perfect tracking control based on multirate feedforward / feedback controllers with generalized sampling periods," in *14th IFAC World Congress*, vol. C, pp. 61–66, July 1999.

[13] H. Fujimoto, A. Kawamura, and M. Tomizuka, "Generalized digital redesign method for linear feedback system based on N-delay control," *IEEE/ASME Trans. Mechatronics*, vol. 4, no. 2, pp. 101–109, 1999.

[14] T. Sugie and T. Yoshikawa, "General solution of robust tracking problem in two-degree-of-freedom control systems," *IEEE Trans. Automat. Contr.*, vol. 31, no. 6, pp. 552–554, 1986.

[15] H. Fujimoto, Y. Hori, T. Yamaguchi, and S. Nakagawa, "Proposal of perfect tracking and perfect disturbance rejection control by multirate sampling and applications to hard disk drive control," in *Conf. Decision Contr.*, pp. 5277–5282, December 1999.

[16] K. Zhou, J. Doyle, and K. Glover, *Robust and Optimal Control*. Prentice-Hall, Inc, 1996.

[17] M. Araki and T. Hagiwara, "Pole assignment by multirate-data output feedback," *Int. J. Control*, vol. 44, no. 6, pp. 1661–1673, 1986.

[18] H. Fujimoto, Y. Hori, and A. Kawamura, "Structure of perfect tracking controller based on multirate feedforward control," in *Int. Power Electronics Conference*, April 2000. (to be presented).

[19] G. F. Franklin and J. D. Powell, *Digital Control of Dynamic Systems*. Addison-Wesley Publishing Company, 1980.

[20] Y. Gu and M. Tomizuka, "High performance tracking control system under measurement constraints by multirate control," in *14th IFAC World Congress*, vol. C, pp. 67–71, July 1999.